Hindawi
Shock and Vibration
Volume 2019, Article ID 6276915, 13 pages
https://doi.org/10.1155/2019/6276915

Research Article

Vibration Analysis of Composite Multilayer Floor of High-Speed Train

Ying Han, Wenjing Sun, Jinsong Zhou, and Dao Gong

Institute of Rail Transit, Tongji University, Shanghai 201804, China

Correspondence should be addressed to Wenjing Sun; sunwenjing19@gmail.com

Received 19 August 2019; Accepted 10 October 2019; Published 31 October 2019

Academic Editor: Nerio Tullini

Mechanical properties of floor prototypes made for high-speed trains from composite multilayer floor structures of different materials and thicknesses were tested. Based on the test results, the equivalent mechanical parameters of different layers of the panels, core materials, etc., were calculated, and the multilayer mixed finite element model of the floor was built and verified. The multilayer mixed floor model was introduced into the car body of a high-speed train, and the test signals of the high-speed train were used as inputs to calculate the vibration response of composite floor structure. Vibration spectra of the high-speed train composite floor made of different materials and structures were compared and analyzed. The results show that the calculation of the floor vibration response of the vehicle car body within the framework of the equivalent model of the multilayer structure based on the mechanical performance test is an effective method to evaluate vibration characteristics. The vibration isolation performance of the stainless steel panel floor is better than that of the aluminum alloy panel, but its large mass is not favorable in lightweight body design. The vibration energy of birch core material floor is significantly smaller than the alder core material of the same size. The vibration isolation performance of the floor enhanced with the increase in the thickness of the outer metal panel, but when the outer metal panel thickness exceeds 0.8 mm, the influence becomes small. Therefore, the stainless steel-birch core composite floor with a large panel thickness has the best vibration isolation performance and can be used for the floor above the bogie and the suspended excitation source. Then, an optimal analysis considering mass and vibration characteristics was carried out, and the results show that there exists an optimal solution for the high-speed train. Regarding the overall design basis of the vehicle, the aluminum alloy panel lightweight structure can be used in combination with other general parts.

1. Introduction

With the rapid development of China's high-speed rail transit system, excellent ride comfort and the safety of train operations are important issues of high-speed train vehicle design. Due to the high speed of the train, the increased excitation energy of wheel and rail interaction and the lightweight design lead to aggravation of the flexible vibration of the vehicle car body structure [1–4]. Therefore, the vibration isolation and attenuation performance of high-speed vehicle structural parts are very important [5]. At present, the low-frequency noise dominates for interior noise of high-speed trains [6]. The structure-borne noise of the vehicle car body is mostly in the low-frequency range. A vibration of the carriage floor structure is the main source of structure-borne noise in a vehicle [7], and the floor medium has an important vibration isolation function between the bogie and interior car body. Passengers contact with the floor directly, and seats are installed on the floor. Therefore, the structural form of the floor and the selection of material parameters have a great influence on the ride comfort of passengers in a vehicle. Reducing vibration of the floor structure can decrease vehicle interior noise as well.

Previously, some scholars investigated floor structure vibration and noise reduction problems. For example, Fan et al. [8] laid different types of damping layers on the exterior floor of a vehicle to reduce the vibration of the interior structure; Zhang et al. [9] designed a floating floor vibration damper to reduce the vibration transmission energy of the vehicle body floor. Miao [10] proposed a composite material

structure as a flooring material to reduce vibration and noise.

Composite materials are widely used in high-speed trains all over the world [11–13]. The use of composite multilayer structures for train floors also becomes increasingly common. Compared with single-layer structures, they are lighter and have better sound isolation properties [14, 15]. The finite element method has proven to be an effective method for analyzing the mechanical properties of composite multilayer structures. A new higher-order layerwise finite element model is built by Belarbi et al. [16], which is suitable for the vibration problem of composite structure. However, in practical applications, the types and sizes of composite structural materials that can be selected are different. The influence and rules of different composite flooring materials and structural distribution on train floor vibration are not yet clear. Based on this, this paper takes 16 kinds of composite multilayer panel floor structures as the research object. Combining experimental and simulation results, composite floor vibration characteristics of a high-speed train were analyzed. Based on test results of the mechanical properties, the equivalent material parameters of the composite structure are calculated. The hybrid multilayer composite floor model was developed and validated. The model of vehicle car body structure containing the multilayer panel car floor was calculated. Using the on-site measured vibration data of the high-speed train car body underframe as the excitation, the vibration characteristics of floors with different composite structures were obtained, which provides a basis for an optimal design of high-speed train floor parameters in the future. Finally, an optimal analysis model is used to find an optimal solution for the design of a composite multilayer floor.

2. Mechanical Properties Test of Composite Multilayer Floor

2.1. Mechanical Properties Test. 16 kinds of floors studied in this paper were typical composite multilayer panel structures. They are composed of metal panels (stainless steel or aluminum alloy), core materials (birch or alder), and a layer of rubber units with different thicknesses. The total thickness of each structure was 22 mm. One of the floor prototypes is shown in Figure 1.

Each composite multilayer panel structure consists of 18 layers bonded together as shown in Figure 2. The upper and lower bottom layers are surface metal panels, the middle black layer is the rubber unit, and the remaining 15 layers are rotated at 90° angle from the grain direction. Wood is made up of different phases, and all layers together form an overall force element. In a multilayer structure, the material, thickness, and main direction of elasticity of every single layer may differ from each other and possess anisotropic characteristics. In order to obtain material parameters of the composite multilayer panel floor structure and to calculate the vibration response of the floor, various types of floor samples were first tested for mechanical properties, and the equivalent calculation of the material parameters based on the test results were used to create a finite element model of the composite multilayer panel floor.

Figure 1: Composite floor sample ($400 \times 60 \times 22\,mm^3$).

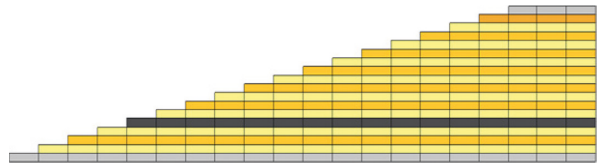

Figure 2: Diagram of composite multilayer panel structure.

The mechanical performance parameters of the composite multilayer floor can be obtained by bending performance tests, compressive strength, and tensile strength tests on samples with different lengths [17–19]. Among them, the bending performance test of the composite multilayer panel structure is shown in Figure 3. According to the bending performance test standard, the bending stiffness and the shear stiffness were measured through the three-point bending test of outrigger samples with multilayer structures [20], as shown in Figure 4. The span of the outrigger is $l = 200$ mm, and the outer elongation is $a = 100$ mm. Thereby, the elastic modulus of the panel structure and the shear modulus of the core structure could be calculated. The compressive strength test and tensile strength test were carried out to obtain the flat pressure value, flat tensile strength, and flat elastic modulus of each floor structure sample.

2.2. Test Results Analysis. The bending stiffness and shear stiffness of the composite multilayer panel structure can be determined by three-point bending of the long panel sample, and the elastic modulus of the panel and the shear modulus of the core material can be calculated. To reduce the error, the results of the mechanical properties of each sample were selected from 5 groups and averaged according to the load-deflection curve data. Taking one sample as an example, the load-deflection curve of the composite multilayer panel structure was plotted, as shown in Figure 5.

From Figure 5, it can be seen that, at the initial loading stage, due to the interference of the test environment and the test instrument error, there was a certain deviation in the load-displacement curve. As the load increased to the range of 500–3500 N, the relationship between the displacement and the load was linear at the centre of the sample. At this time, the floor structure deformation relates to the linear part of the curve. When the load continues to increase, due to the oversized load and deformation of the sample, the property of the structure enters into the nonlinear region. Considering the fact that the deformation of the floor structure is smaller at actual vibrations and within the linear range, the nonlinear property was not taken into account during the calculation. According to the load-deflection

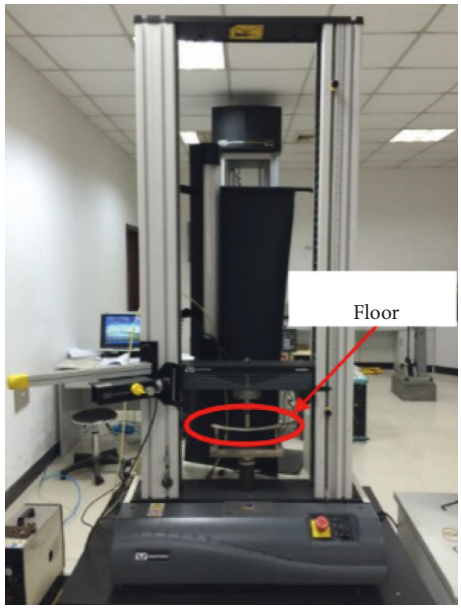

Figure 3: Composite multilayer panel bending test.

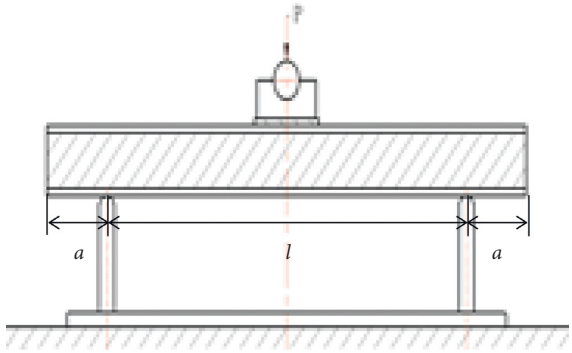

Figure 4: Three-point bending test device.

curve of the composite multilayer panel structure test, parameters such as bending stiffness, elastic modulus, and shear modulus of the composite multilayer panel floor samples can be obtained through calculation [17].

The bending rigidity of the overall structure of the composite multilayer panel sample can be obtained by the following equation:

$$D = \frac{\Delta p l^3 a}{16\delta}, \tag{1}$$

where D is the flexural rigidity of the sample and the unit is N·mm^2; l is the three-point bending span and the unit is mm; a is the length of the outrigger beam and the unit is mm; Δp is the load increment value on the load-deflection curve and the unit is N; and δ is the deflection of the sample's extensibility that corresponds to the Δp load and the unit is mm. The elastic modulus of the sample panel structure can be obtained by the following equation:

$$E_t = \frac{D}{J}, \tag{2}$$

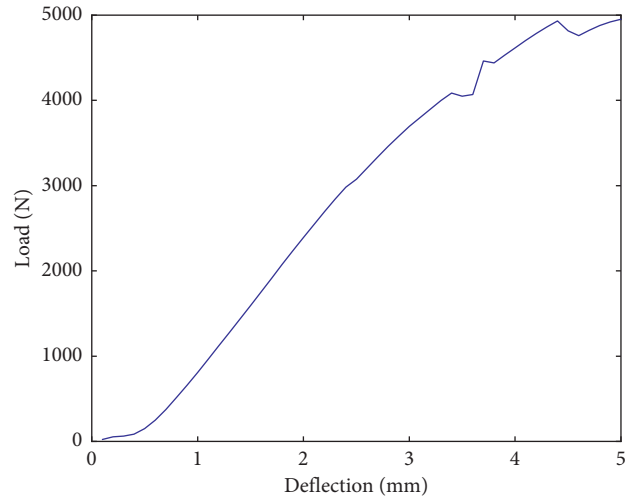

Figure 5: Bending load-deflection curve.

where J is the moment of inertia of the multilayer panel structure and the unit is mm^4.

The shear stiffness U of composite multilayer panel samples was calculated as follows:

$$U = \frac{\Delta p l}{4\left(\delta_c - (l/3a) \times \delta\right)}, \tag{3}$$

where the shear stiffness unit is N and δ_c is the increase of deflection at the centre of the sample and the unit is mm.

The shear modulus of the core material can be calculated from the following equation:

$$G_s = \frac{U}{b\left(h - t_1\right)}, \tag{4}$$

where b is the sample width, h is the sample thickness, and t_1 is the surface panel thickness in mm.

After the above tests and calculations, the structural mechanical properties and material property parameters of 16 kinds of composite multilayer panel structure samples are listed in Table 1 including the overall bending stiffness and shear stiffness of the multilayer panel floor structure and the structural elastic modulus of the panel, the shear modulus of the core material, and the bending, flat pressure, and flat tensile strength of the floor sample.

3. Design and Verification of Car Body Floor Model

3.1. Composite Floor Structure Modeling. The finite element model of the composite floor was established according to the structural geometry parameters of the panel and the core material properties, such as the elastic modulus, shear modulus, and other material parameters. The input parameters include the density, elastic modulus, and Poisson ratio of the multilayer panel structure. In the modeling of multilayer composite structures, a hybrid model is used to divide the composite structure into several layers [21]. Each layer has different material properties, and different types of

Table 1: Test and calculation results of mechanical properties of composite multilayer panels.

Material code	Panel material	Core material	Panel thickness (mm)	Density (t/mm^3)	Bending stiffness ($N{\cdot}mm^2$)	Shear stiffness (N)	Panel elastic modulus (MPa)	Core shear modulus (MPa)	Flat modulus (MPa)
1	Aluminum	Birch	0.5	$1.07e-09$	$6.78e8$	$1.26e5$	$6.32e4$	95.4	206
2			0.8	$1.08e-09$	$6.22e8$	$1.51e5$	$4.15e4$	115	280
3			1.0	$1.10e-09$	$7.60e8$	$1.57e5$	$4.33e4$	118	196
4			1.5	$1.12e-09$	$8.27e8$	$3.74e4$	$3.74e4$	94.8	339
5		Alder	0.5	$7.67e-10$	$3.59e8$	$6.56e4$	$3.54e4$	51.0	169
6			0.8	$8.62e-10$	$3.79e8$	$7.52e4$	$2.63e4$	58.1	167
7			1.0	$8.71e-10$	$3.91e8$	$8.20e4$	$2.29e4$	62.6	169
8			1.5	$8.99e-10$	$3.81e8$	$8.17e4$	$1.74e4$	61.6	193
9	Stainless steel	Birch	0.5	$1.44e-09$	$1.03e9$	$1.54e5$	$9.84e4$	117.0	254
10			0.8	$1.61e-09$	$1.04e9$	$1.59e5$	$7.02e4$	121.0	253
11			1.0	$1.69e-09$	$1.10e9$	$1.68e5$	$6.28e4$	127.0	284
12			1.5	$1.88e-09$	$9.42e8$	$1.59e5$	$4.27e4$	119.0	255
13		Alder	0.5	$1.28e-09$	$4.41e8$	$8.55e4$	$4.33e4$	66.0	129
14			0.8	$1.38e-09$	$4.92e8$	$9.07e4$	$3.36e4$	69.3	168
15			1.0	$1.42e-09$	$4.98e8$	$8.34e4$	$2.91e4$	63.2	201
16			1.5	$1.62e-09$	$4.91e8$	$8.48e4$	$2.29e4$	64.8	125

unit simulations can be selected. The multilayer panel flooring studied in this paper contains three types of material units: metal panels (stainless or aluminum), wood (birch or alder), and rubber. In a real environment, the deformation of the floor structure is small and within the linear range. Therefore, metal panels and wood layers are simplified to isotropic linear materials. The rubber is regarded as a superelastic material and modeled by using the Mooney–Rivlin model [22]. The finite element software Abaqus is suitable for multilayer structure modeling and convenient for solving structural deformation problems of rubber materials, so it is used to design a multilayer mixed model of multilayer panels as shown in Figure 6. In order to introduce the multilayer mixed floor model into the car body of a high-speed train, an equivalent two-dimensional model consisting of shell elements was also established. The section properties were set according to the equivalent material parameters calculated in Section 2.2, as shown in Figure 7.

To verify the finite element model of the composite multilayer floor, the models were loaded and simulated as the simulated mechanical performance test. The loading and supporting methods of the actual floor model were the same as those of the prototype test, while the equivalent model applied the constraints and loads on nodes, shown in Figure 7.

The overall structural load-deflection curve of the multilayer mixed model is shown in Figure 8. It can be seen that the calculation results of the bending characteristics of the two finite element models and the test results are all linear in the 500–3000 N load range. In the same way, when the floor vibration analysis was performed, it was mainly considered within the linear elastic deformation range. Meanwhile, compared with the actual floor model, the equivalent model is easier to model, and the calculation amount is smaller. Therefore, the results of the bending stiffness of the equivalent floor model are consistent with the test results, and the model can be used for the calculation of the floor vibration characteristics at the next step.

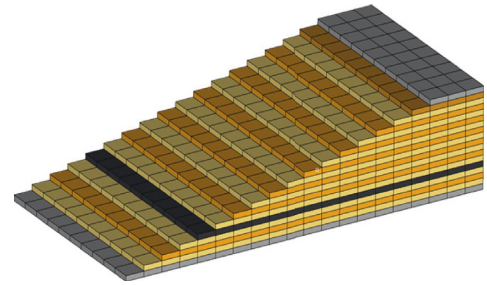

Figure 6: Composite multilayer floor structure model.

Based on the equivalent model of the 18-layer hybrid floor established with the above method, the finite element model of the loading structure in the sightseeing area was designed and introduced into the vehicle car body model to calculate the vibration isolation performance of the vehicle floor structure. The sightseeing area locates between the normal passenger compartment and driver's cab.

3.2. FEM Model of Car Body with Floor Structure. The first car of a high-speed train is taken as the research object here, and it includes three parts: the driver's cab, the sightseeing area, and the car body carrying structure. Based on the three-dimensional geometric structure, the finite element model of the vehicle car body was designed. To ensure the calculation accuracy and increase the calculation efficiency, the model calculation amount is appropriately considered. The finite element model including the interior structure is built in the passenger compartment of the sightseeing area, including the top roof panel, the partition, the middle roof panel, and the floor. In the four parts, the floor structure of the sightseeing area is calculated and analyzed in detail, while the other parts such as the passenger compartment and driver's cab adopt the bearing structure that does not include the detailed floor model. In the finite element model, the car

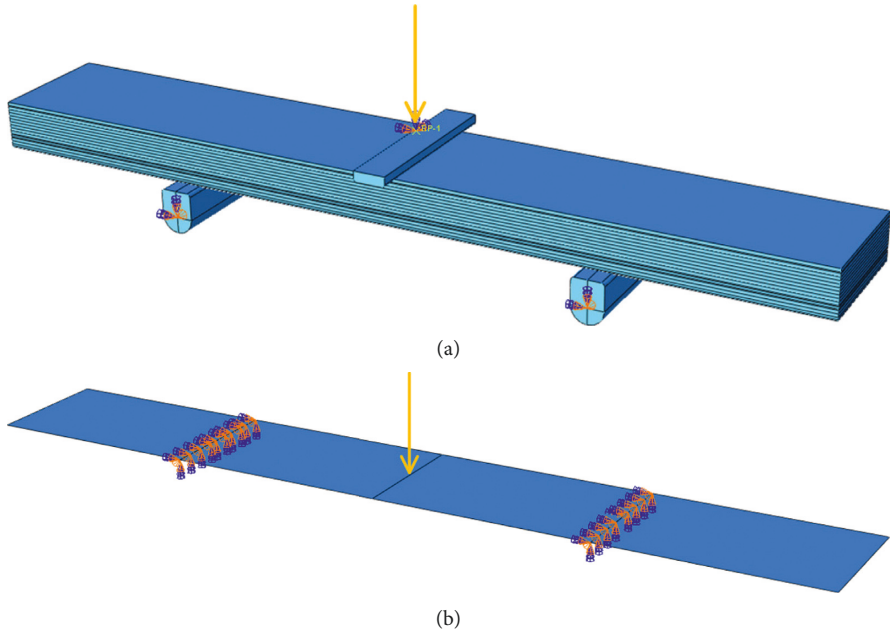

(a)

(b)

Figure 7: Loading simulation of floor model. (a) Multilayer mixed model. (b) Equivalent model.

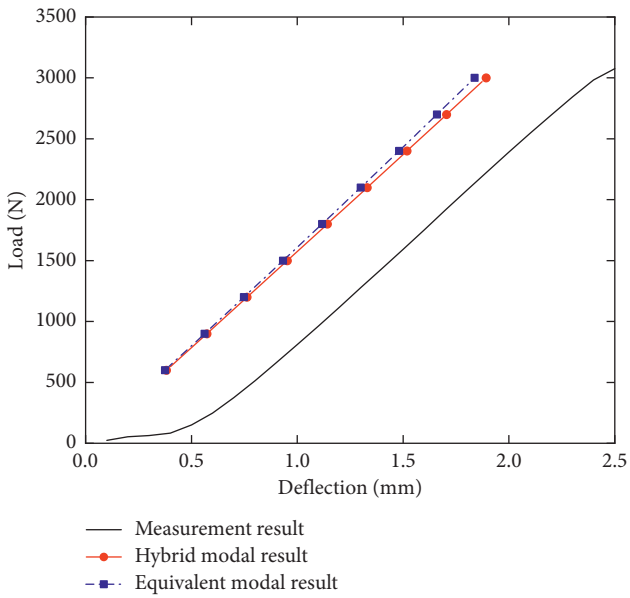

Figure 8: Comparison of the bending property of the floor models and test result.

body is a plate structure that is simulated with shell elements and discrete by four-node shell elements.

In the sightseeing area, a rubber damping element is installed between the floor and the aluminum alloy underframe of the floor structure of the car body. The spring damping unit is used here to simulate the stiffness and damping property. The top roof panel, side wall panel, and the aluminum alloy underframe body are fixed with bolts, so the rigid connection units are used here. The finite element model of a high-speed train head carriage body consists of 320,928 nodes and 414,222 elements. The sightseeing area model is assembled with other parts of the first vehicle body structure. The finite element model of the vehicle body and the sightseeing area is shown in Figure 9.

To calculate the vibration response of the floor including the multilayer panel hybrid model, the response output points were set in the floor model of the sightseeing area.

4. Composite Multilayer Panel Floor Vibration Analysis

4.1. Vehicle Vibration Test on Site. According to UIC (International Union of Railways) Standard UIC513 guidelines for evaluating passenger comfort in relation to vibration in railway vehicles [23], the weighted frequency range is up to 40 Hz for lateral and vertical directions. The structure-borne noise from the floor is less than 200 Hz. Thus, the result in this paper is up to 160 Hz for ride comfort and structure vibration.

As to obtain the vibration excitations for the response calculation of the floor, an on-site high-speed train vibration measurement was performed. The acceleration values of car body underframe at the position of air spring seat beam were recorded, which are used as the input signals for calculating the vibration response of floor.

When the vehicle was running at a speed of 350 km/h, the measured vibrations of lateral and vertical accelerations at the bolster beams at time domain are shown in Figure 10. As can be seen from the figure, the vertical vibration signal of the car body underframe of the high-speed train is significantly greater than its lateral vibration. The vibration excitation in frequency domain is shown in Figure 11, which is dominant at low frequencies. With this as input, both vertical and lateral vibration excitations were set at the joint location between the air spring and the vehicle car body to calculate the interior floor vibration characteristics.

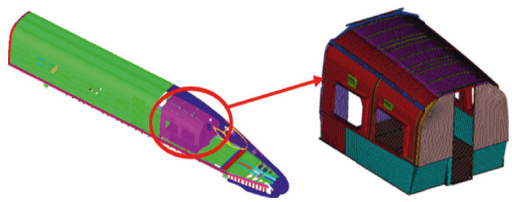

Figure 9: Finite element model of the vehicle body and the sightseeing area.

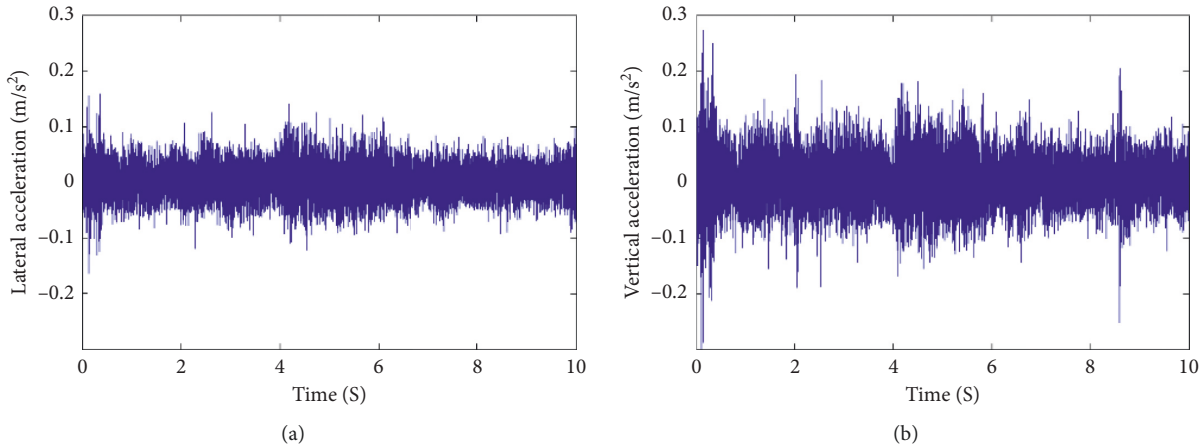

Figure 10: Acceleration data of car body underframe in time domain (350 km/h). (a) Lateral. (b) Vertical.

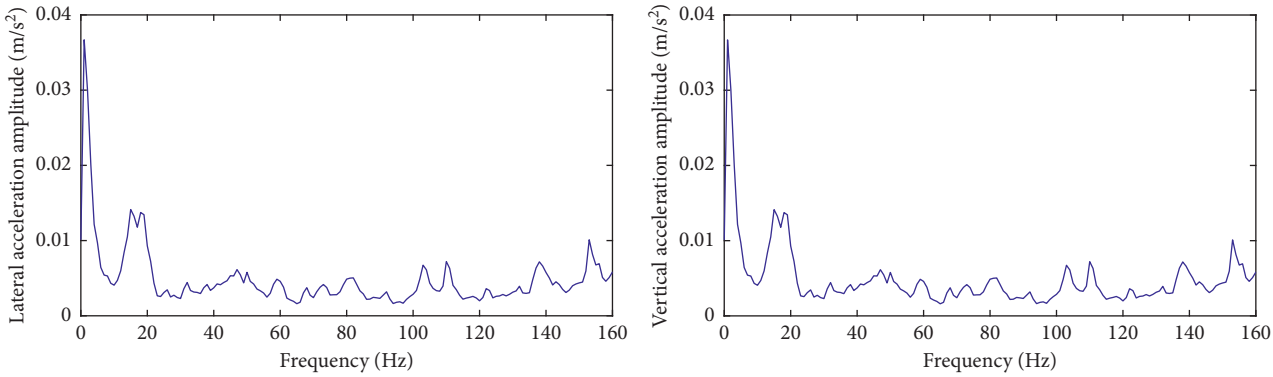

Figure 11: Acceleration data of car body underframe in frequency domain (350 km/h).

4.2. Effect of Surface Panel Material and Thickness on Floor Vibration. The vibration accelerations of the car body underframe at the position of the air spring when the vehicle is running at 350 km/h were taken as the excitations; the floor panel models with different composite multilayer panel structures in Table 1 are selected for transient response analysis, and the floor surface panels with different materials and thicknesses of the 1st–16th composite floor are compared. The comparison of the time domain results of the vertical vibration response at the measuring point is shown in Figure 12. It can be seen that, under the condition of the same core material and panel thickness, both the RMS value and the maximum acceleration of the vibration of the stainless steel panel structure are significantly smaller than the aluminum alloy panel.

Figure 13 shows the results of the frequency domain analysis of different multilayer panel floors. There are vibration peaks near 35 Hz, 58 Hz, 92 Hz, and 150 Hz for different material structures. The vibration energy is higher in these frequency ranges. In Figure 11, there are no peaks from the excitation point. The vibration peaks should be due to the floor structure itself. It can be seen from Figures 12 and 13 that as the thickness of the metal surface panel increases, the vibration acceleration decreases. When the thickness of the metal panel is 0.5 mm, the vibration acceleration value is relatively large. When the thickness is increased to 0.8 mm, the overall floor panel rigidity increases. However, when the aluminum alloy panel thickness was increased to 1.5 mm, the vibration acceleration changes were negligibly small. While the stainless steel panel reduces

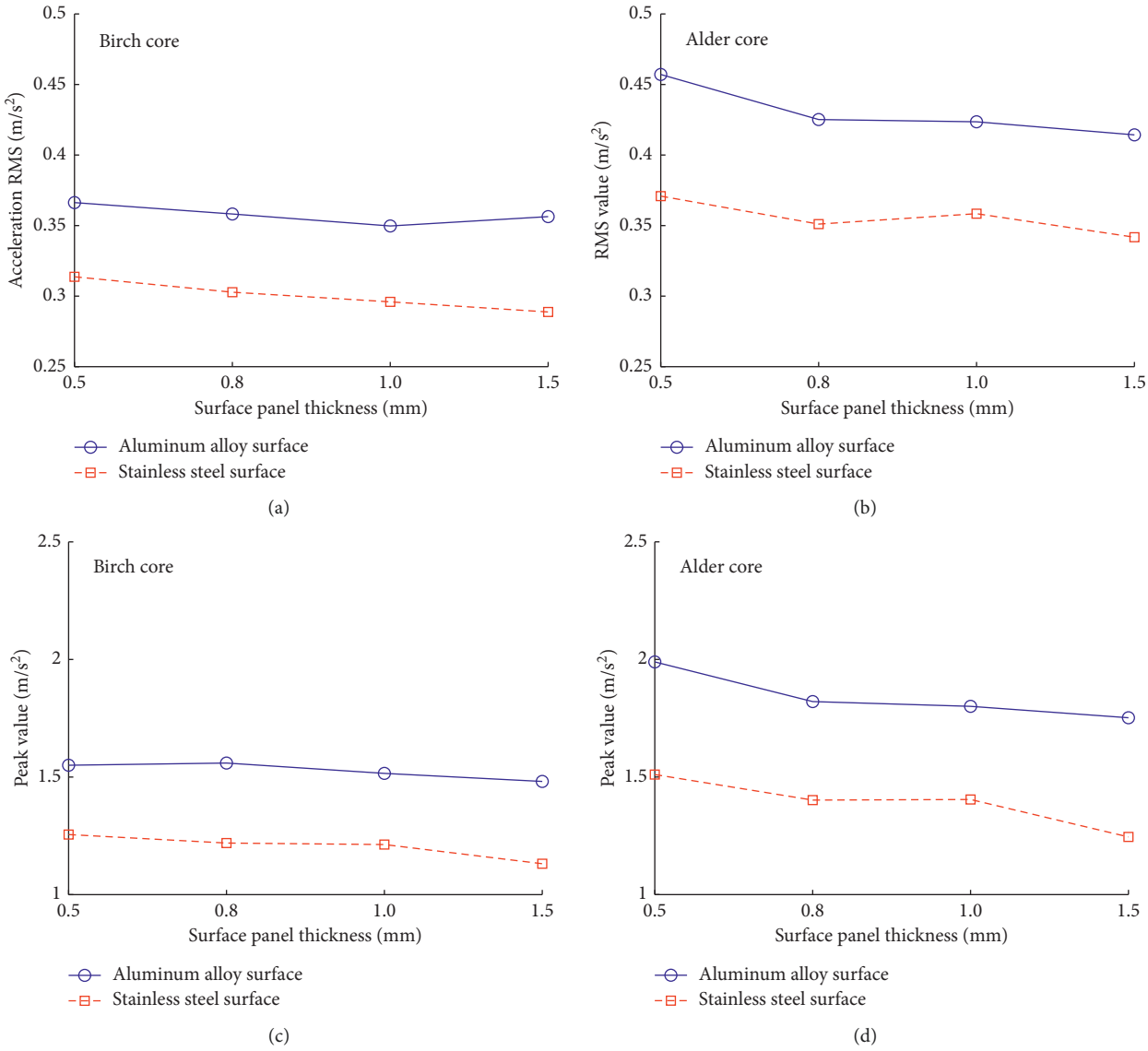

Figure 12: Time domain results of vibration acceleration response. (a) Vibration RMS value of birch core panels. (b) Vibration RMS value of alder core panels. (c) Vibration peak value of birch core panels. (d) Vibration peak value of alder core panels.

the high-frequency vibration energy after 30 Hz, the low-frequency vibration energy increases, and also, the weight of the floor increases. Based on comprehensive considerations, the panel thickness of 0.8 mm is the best.

Figures 14–16 show the modal analysis results of underframe of car body and floor, respectively. From the figures, it can be seen that for the modal frequencies of 35 Hz, 58 Hz, and 92 Hz, there are no obvious local modes for underframe structure but obvious local modes for floor. The response peaks at these frequencies are mainly due to local modes of floor structure.

4.3. Influence of the Core Material on Floor Vibration. As one may see in Figure 17, the floor acceleration response of the birch core material is smaller than that of the alder wood flooring of the same size and the floor of the same metal surface panel material. The increase in the thickness of the panel has less effect on the vibration of the birch core floor than the alder wood floor.

The comparison of different core materials and panel materials response in the frequency domain is shown in Figure 18. For the same material and the thickness of the surface panel, it can be seen on the entire frequency band that the vibration acceleration of the multilayer panel of the birch core material is significantly less than the alder wood floor, so the birch is selected for better isolation and attenuation of vibration. The core material is conducive to floor vibration damping. At the same time, the vibration of the stainless steel floor structure in the low-frequency region within 30 Hz is slightly larger than that of the aluminum alloy panel structure. The theory of vibration isolation [24] shows that this is because the mass of the stainless steel material is relatively large, and the overall natural frequency

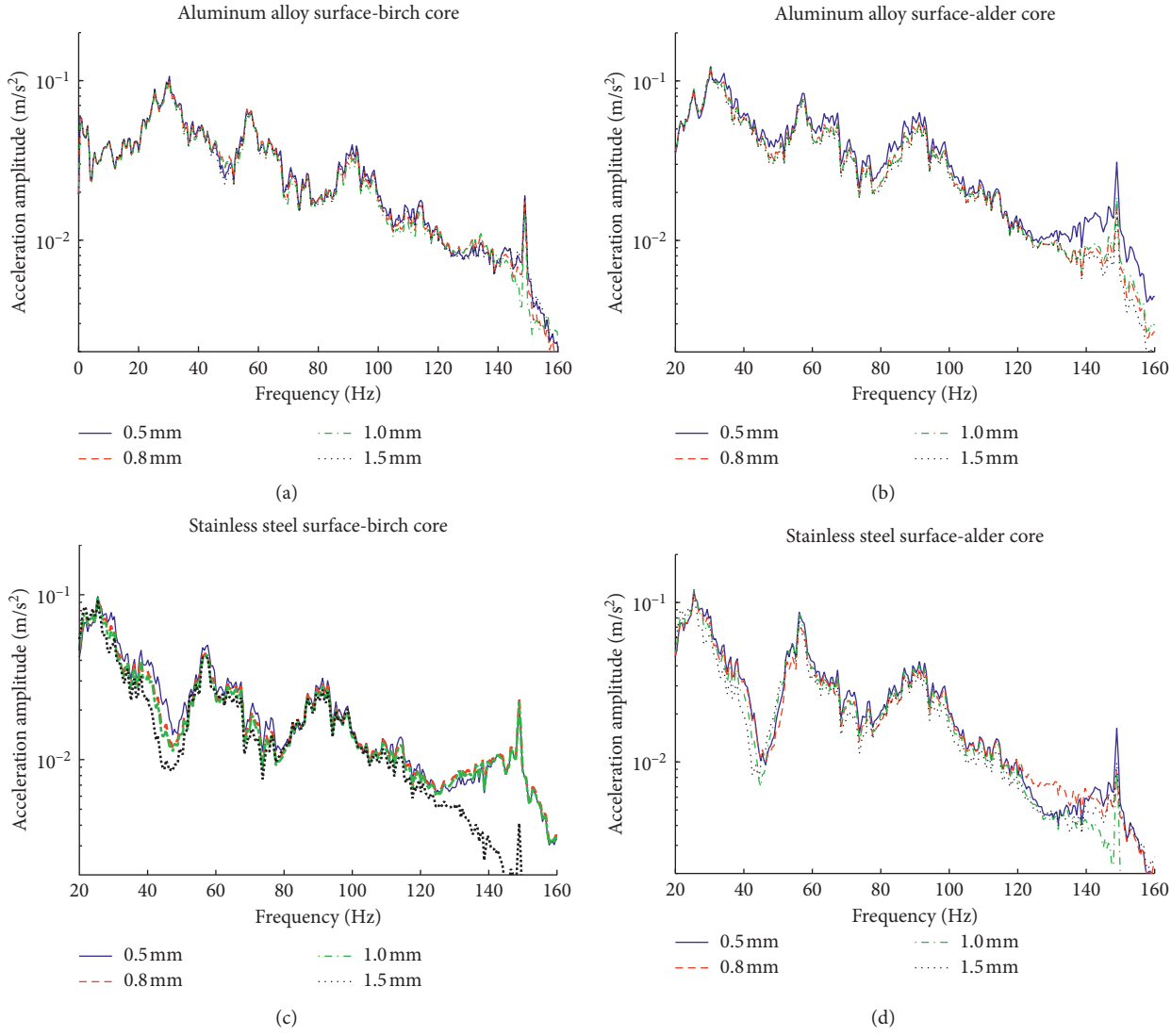

Figure 13: Time domain results of the vibration acceleration response. (a) Aluminum alloy with the birch core material. (b) Aluminum alloy with the alder core material. (c) Stainless steel with the birch core material. (d) Stainless steel with the alder core material.

of the structure is lower than the aluminum alloy panel floor. Therefore, the low-frequency vibration energy is larger. The aluminum alloy panel material, due to its low stiffness, has a significantly higher vibration above 30 Hz than the stainless steel panel floor. Considering the entire frequency domain, the overall vibration isolation performance of stainless steel panels is better than that of aluminum alloy panels. However, considering the lightweight design of the vehicle body, the quality of aluminum alloy panels is better due to its lighter weight.

5. Optimal Analysis of Composite Multilayer Floor

The accuracy of the refined model was verified by the experimental data. Then, a simplified model, which was suitable for analyzing the vibration of a high-speed train, was obtained through the model equivalent method in this paper. However, it is still unable to determine the optimal configuration of different materials and different thickness of composite layers. In order to obtain the optimal parameters, the parameter optimization of the model was carried out as follows.

5.1. Optimum Design. There are many mathematical methods that could be used to solve the optimization problem involving continuous design variables. However, it is not suitable for many practical problems [25]. For the sake of solving this problem, the composite multilayer floor structure would be optimized by using the discrete optimization method.

The design variables and their feasible region for this study are shown in Table 1. The panel thickness δ_q was sampled as discrete arrays, and then, δ_q was combined with floor metal materials P_i and composite layer materials C_j. Finally, 16 sets of design variables could be obtained.

The sets of design variables could be represented by vector x:

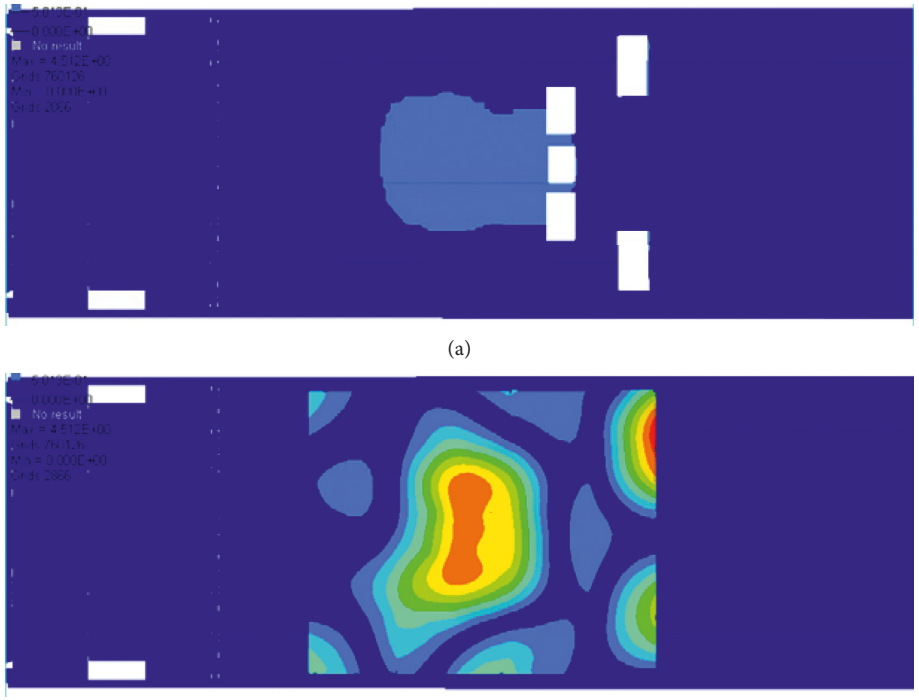

(a)

(b)

Figure 14: Modal shape comparison between (a) underframe of car body (35.25 Hz) and (b) floor .

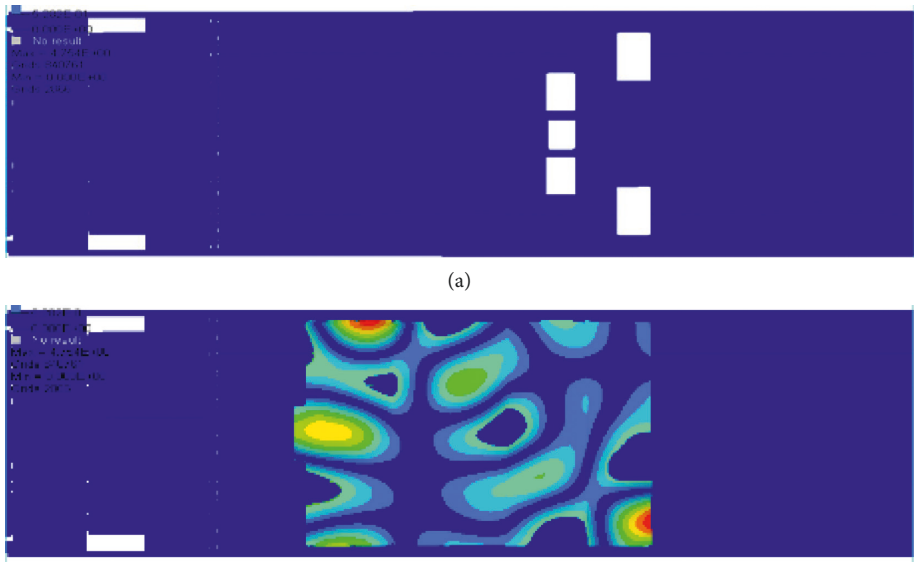

(a)

(b)

Figure 15: Modal shape comparison between (a) underframe of car body (58 Hz) and (b) floor.

$$x = \left(P_i, C_j, \delta_q\right)^T. \tag{5}$$

For high-speed rail vehicles, passenger ride comfort and body weight are both important indicators, which should be taken into consideration in this optimal design. The floor vibration acceleration RMS value can be used to evaluate the ride comfort. The weight of the composite floor can be used to evaluate the lightweight design of the car body.

In order to transform this multiobjective optimization problem into a single-objective optimization problem, the objective function $R(x)$ is defined as follows:

$$R(x) = \alpha A(x) + \beta M(x). \tag{6}$$

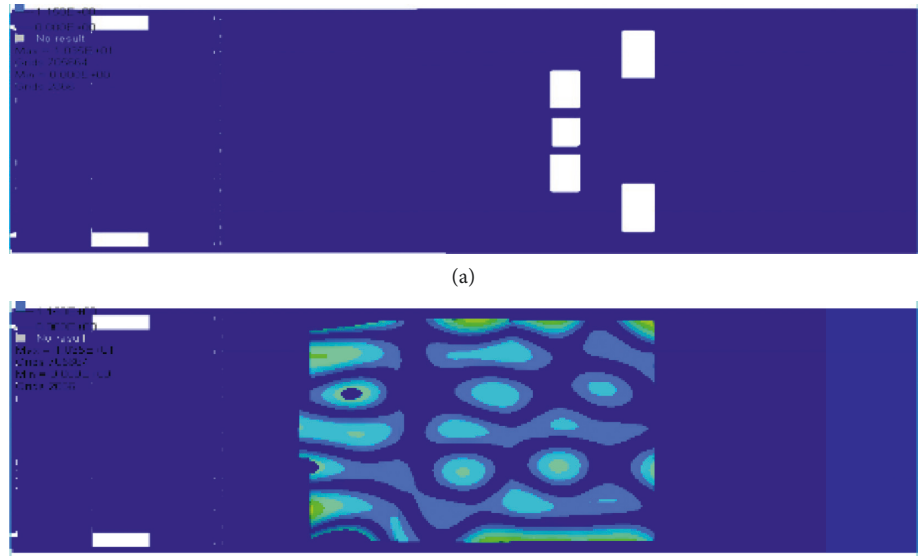

(a)

(b)

Figure 16: Modal shape comparison between (a) underframe of car body (92 Hz) and (b) floor.

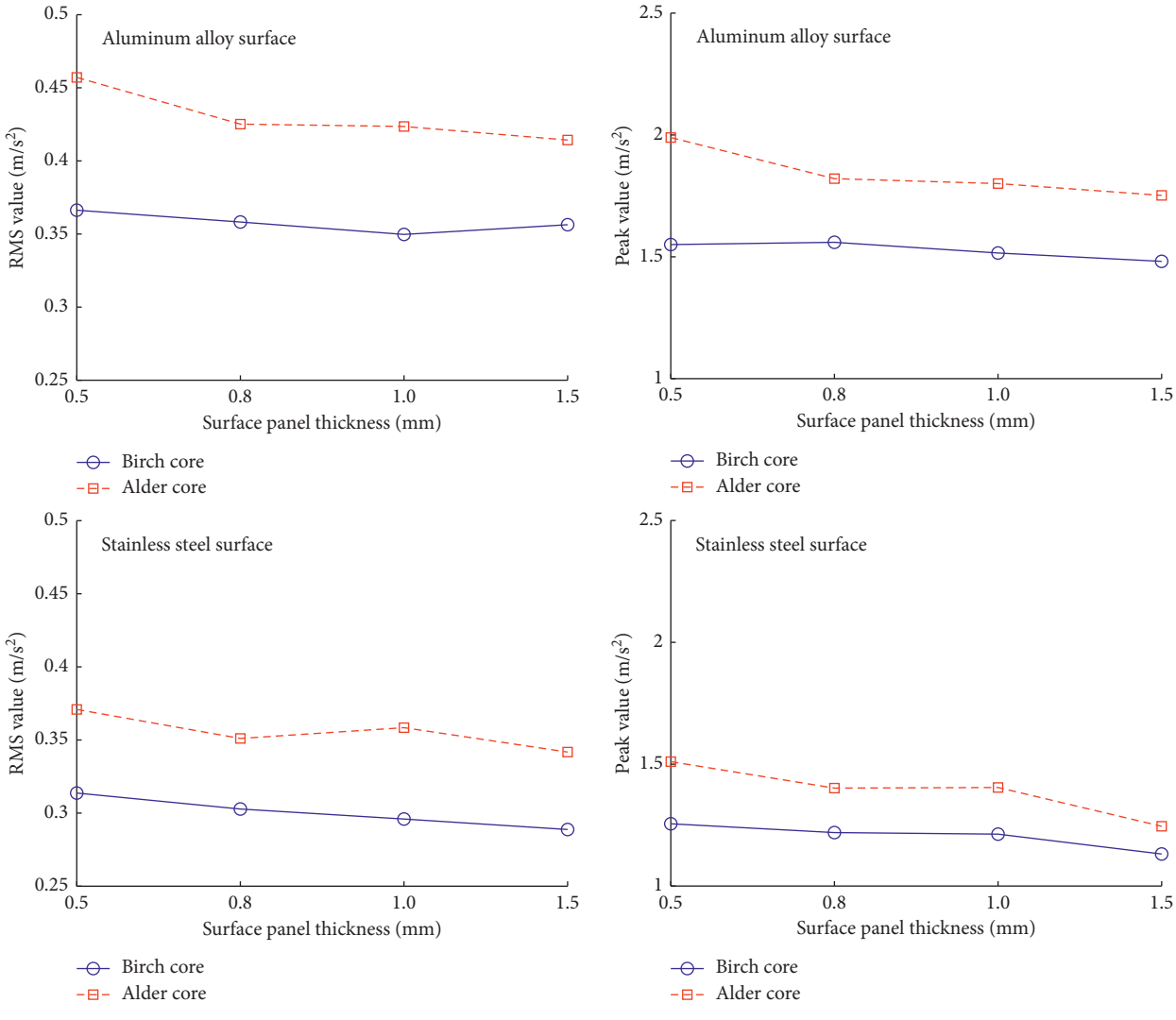

(a) (b)

Figure 17: Vibration acceleration response in time domain. (a) RMS values. (b) Peak values.

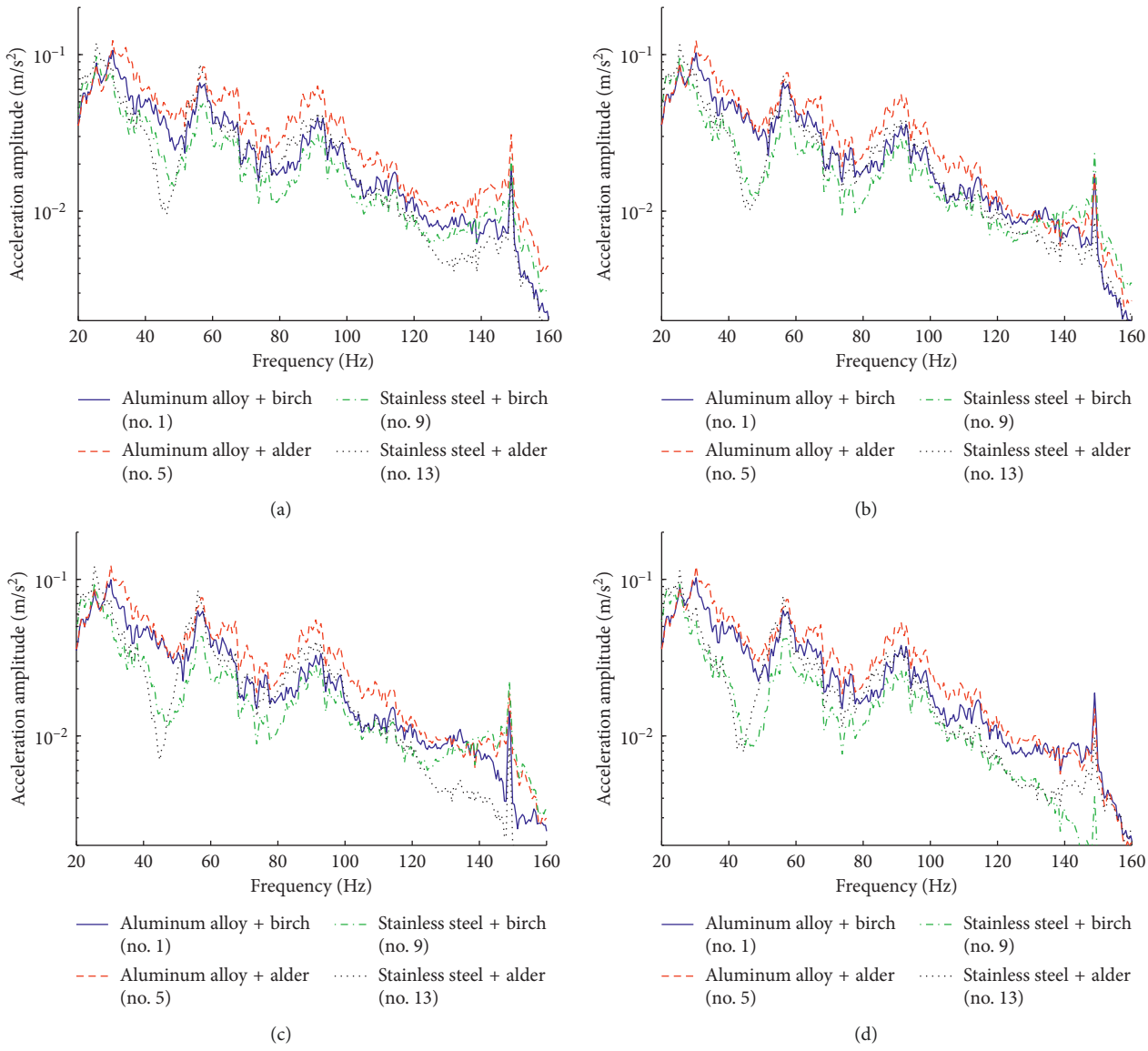

FIGURE 18: Time domain results of the vibration acceleration response. Panel thickness of (a) 0.5 mm; (b) 0.8 mm; (c) 1.0 mm; and (d) 1.5 mm.

where $A(x)$ is the RMS value of floor vibration acceleration after normalization and $M(x)$ is the mass of the composite floor after normalization. α and β are weight coefficients and α and $\beta = 0.5$.

The following optimization mathematical models can express the above optimization problems:

$$\begin{cases} \text{find}: \ x = \left(P_i, C_j, \delta_q\right)^T, \\ \text{minimize}: \ R(x). \end{cases} \tag{7}$$

The flowchart of the optimization analysis is shown in Figure 19.

5.2. Analysis of Optimization Results. The objective function values of 16 sets of design variables are calculated and shown in Figure 20.

From Figure 20, we can see that

(1) Compared with the other three combinations, aluminum-birch has a lower objective function value, which indicates that aluminum-birch is more suitable for high-speed trains when considering the lightweight design of the car body and ride comfort.

(2) When the panel thickness is 1.0 mm in the aluminum-birch combination, the objective function value is the global optimal solution. Therefore, we could

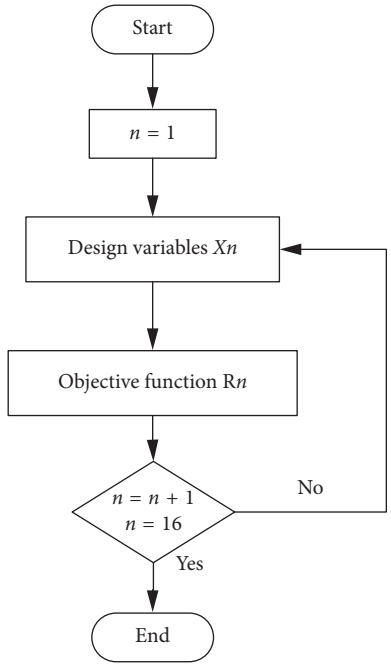

Figure 19: Flowchart of optimization analysis.

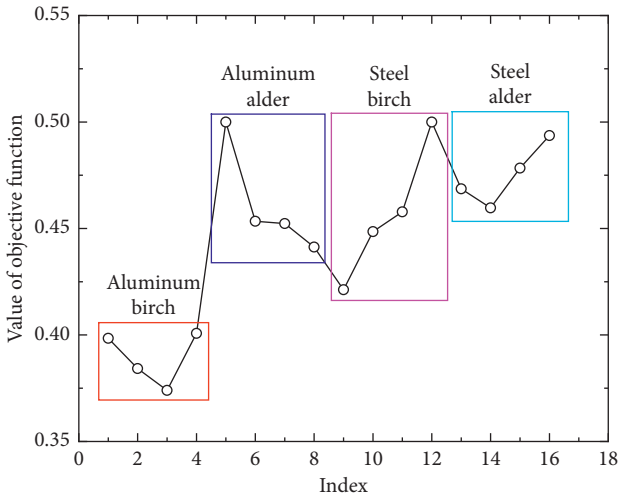

Figure 20: Optimal objective values under different design variables.

get the optimal design variable set, aluminum-birch-1.0 mm. It means that this combination of variables takes into account the advantages of aluminum and birch together.

6. Conclusion

The mechanical properties of different composite multilayer panel floors were measured, and the mechanical characteristic parameters of the multilayer floor material were calculated based on the measurement results. The composite floor structure can be established with the finite element model. A vehicle car body model with a multilayer floor in the sightseeing area was built and measured by vibration signals of the high-speed train running on the track to analyze the vibration characteristics of different composite structures and materials. The vibration performance evaluation of composite multilayer floor structures with different multilayers can be carried out effectively. The calculation results show that the peak vibration frequency of the stainless steel panel is slightly lower than that of the aluminum alloy panel, but the overall stiffness is high, and the vibration isolation performance at high frequencies is good. For the core material, the vibration acceleration of the birch core is significantly lower than that of the alder core material. When the panel thickness was increased from 0.5 mm to 0.8 mm, the interior vibration energy of the floor surface reduced, and the effect of a continued increase in thickness is smaller. Based on comprehensive consideration of the magnitude of vibration acceleration, frequency domain distribution of the vibration energy and floor structure quality difference, stainless steel panel (0.8 mm) + birch core composite wood material flooring structure can be used above the bogie and for the car body parts with high vibration isolation requirements, while other common parts can use aluminum alloy (0.8 mm) + birch core structure due to the lightweight design of a high-speed train. The vibration and lightweight design are considered as two optimization objectives, aluminum-birch-1.0 mm is the optimal combination for the high-speed train through optimization analysis.

Data Availability

The data used to support the findings of this study are available from the corresponding author upon request.

Conflicts of Interest

The authors declare that they have no conflicts of interest.

Acknowledgments

The authors acknowledge the financial support provided by the National Natural Science Foundation of China (grant no. 51805373).

References

[1] T. Tomioka, Y. Suzuki, and T. Takigami, "Three-dimensional flexural vibration of lightweight railway vehicle carbody and a new analytical method for flexural vibration," *Quarterly Report of RTRI*, vol. 44, no. 1, pp. 15–21, 2003.

[2] T. Yamaguchi, Y. Kurosawa, S. Matsumura, and A. Nomura, "Finite element analysis for vibration properties of panels in car bodies having viscoelastic damping layer. 1st reprot. Comparison of damping properties," *Transactions of the Japan Society of Mechanical Engineers Series C*, vol. 69, no. 678, pp. 297–303, 2003.

[3] G. Xie, *The Vibroacoustic Behavior of Aluminum Extrusions Used in Railway Vehicles*, University of Southampton, Southampton, UK, 2004.

[4] D. Gong, J. Zhou, W. Sun et al., "Analysis of coupling vibration of elastic body and bogie of high-speed trains,"

Journal of Transportation Engineering, vol. 11, no. 4, pp. 41–47, 2011, in Chinese.

[5] Y. Hong, "Research on damping and noise reduction technologies for high speed trains," *Rolling Stock*, vol. 44, no. 2, pp. 9–15, 2006, in Chinese.

[6] D. Thompson, *Railway Noise and Vibration: Mechanisms, Modeling, and Means of Control*, Elsevier, Amsterdam, The Netherlands, 2008.

[7] Y. Yu, X. Xiao, D. Wang et al., "Prediction of interior structure-borne noise of a cabin of high speed train using FE-SEA hybrid methods," in *Proceedings of the INTER-NOISE and NOISE-CON Congress and Conference*, vol. 2011, no. 4, pp. 3073–3078, Institute of Noise Control Engineering, Osaka, Japan, September 2011.

[8] R. Fan, G. Meng, J. Yang, and C. He, "Experimental study of the effect of viscoelastic damping materials on noise and vibration reduction within railway vehicles," *Journal of Sound and Vibration*, vol. 319, no. 1-2, pp. 58–76, 2009.

[9] Y. Zhang, M. Wang, and M. Sun, "Design method of floor damper on high-speed trains," *Science and Technology Innovation Herald*, no. 19, pp. 57-58, 2013, in Chinese.

[10] X. Miao, "Analysis and control methods of inner noise of high speed train," *Chemical Engineering & Equipment*, no. 4, pp. 202-203, 2010, in Chinese.

[11] K. B. Shin and S. H. Hahn, "Evaluation of the structural integrity of hybrid railway carriage structures including the ageing effects of composite materials," *Composite Structures*, vol. 68, no. 2, pp. 129–137, 2005.

[12] A. Zinno, E. Fusco, A. Prota, and G. Manfredi, "Multiscale approach for the design of composite sandwich structures for train application," *Composite Structures*, vol. 92, no. 9, pp. 2208–2219, 2010.

[13] Z. Wu, J. Zeng, and J. Liu, "Development of high-speed train and its composites," *Materials Review*, no. 21, pp. 108–114, 2011, in Chinese.

[14] T. E. Vigran, "Sound transmission in multilayered structures-introducing finite structural connections in the transfer matrix method," *Applied Acoustics*, vol. 71, no. 1, pp. 39–44, 2010.

[15] M. Villot, C. Guigou, and L. Gagliardini, "Predicting the acoustical radiation of finite size multi-layered structures by applying spatial windowing on infinite structures," *Journal of Sound and Vibration*, vol. 245, no. 3, pp. 433–455, 2001.

[16] M.-O. Belarbi, A. Tati, and H. O. A. Khechai, "On the free vibration analysis of laminated composite and sandwich plates: a layer wise finite element formulation," *Latin American Journal of Solids and Structures*, vol. 14, no. 12, pp. 2265–2290, 2017.

[17] GB/T1456-2005, *Test Method for Flexural Properties of Multilayer Constructions*, Standards Press of China, Beijing, China, 2005, in Chinese.

[18] GB/T1453-2005, *Test Method for Flatwise Compression Properties of Nonmetal Multilayer Constructions or Cores*, Standards Press of China, Beijing, China, 2005, in Chinese.

[19] GB1452-2005, *Test Method for Flatwise Tension Strength of Nonmetal Multilayer Constructions*, Standards Press of China, Beijing, China, 2005, in Chinese.

[20] G. Sun, S. Tong, D. Chen, Z. Gong, and Q. Li, "Mechanical properties of hybrid composites reinforced by carbon and basalt fibers," *International Journal of Mechanical Sciences*, vol. 148, pp. 636–651, 2018.

[21] D. Chen, G. Sun, M. Meng, X. Jin, and Q. Li, "Flexural performance and cost efficiency of carbon/basalt/glass hybrid FRP composite laminates," *Thin-Walled Structures*, vol. 142, pp. 516–531, 2019.

[22] R. S. Rivlin and K. N. Sawyers, "The strain-energy function for elastomers," *Collected Papers of R.S. Rivlin*, pp. 405–417, Springer, Berlin, Germany, 1997.

[23] International Union of Railways and European Committee for Standard, *UIC Code 513 Guideline for Evaluation Passenger Comfort Relation to Vibration in Railway Vehicles*, International Union of Railways (UIC) and European Committee for Standard (CEN), Paris, France, 1994.

[24] S. Rao and F. Yap, *Mechanical Vibrations*, Addison-Wesley, Boston, MA, USA, 1995.

[25] G. Sun, H. Yu, Z. Wang, Z. Xiao, and Q. Li, "Energy absorption mechanics and design optimization of CFRP/aluminium hybrid structures for transverse loading," *International Journal of Mechanical Sciences*, vol. 150, pp. 767–783, 2019.